Influence of the carbon support on the Pt-Sn anodic catalyst for the electrochemical reforming of ethanol

A. B. Calcerrada, A. R. de la Osa, E. Lopez-Fernandez, F. Dorado, A. de Lucas-Consuegra*

Departamento de Ingeniería Química, Facultad de Ciencias y Tecnologías Químicas, Universidad de Castilla-La Mancha, Avenida Camilo José Cela 12, 13071 Ciudad Real, Spain.

*Corresponding author. Tel.: +34-926295300; Fax: +34-926295437; E-mail address: Antonio.Lconsuegra@uclm.es

ABSTRACT

Several anodic catalysts based on Pt-Sn (3:1 mass ratio) and 20% total metal loading were prepared on different carbonaceous supports (functionalized and non-functionalized low-density nanofibers, graphite oxide, expanded graphite, graphene flakes and β-SiC), to identify an alternative for the traditional Carbon Vulcan XC-72 support for the electrochemical reforming of ethanol. Of the materials tested, Pt-Sn supported on non-functionalized low-density nanofibers (CNF LS) showed the highest electro-catalytic activity vs. the traditional support. This result was attributed to the combination of different properties such as high surface area and dispersion of the Pt-Sn nanoparticles, high electrochemical active surface area and high basicity. This anodic catalyst was chosen for the development of a Membrane Electrode Assembly (MEA) and tested for the electrochemical reforming of ethanol. A high activity was obtained (120 $mA \cdot cm^{-2}$ at 1.4 V and 80 ºC) for hydrogen production. In addition, the stability of the system and its subsequent regeneration were studied in view of its practical application.

KEYWORDS

H_2 production; Electrolysis; Electrochemical reforming; Pt-Sn-anode; carbonaceous-supports

1. Introduction

The increase in the total world energy consumption and the limitation of fossil fuel reserves have led to hydrogen being highlighted as the most promising energy carrier to provide a clean, reliable and sustainable energy system [1-3]. Although hydrogen can be produced using different techniques (steam reforming, partial oxidation and electrolysis, amongst others), water electrolysis is known to be one of the most widely used alternatives since it generates pure hydrogen in a single step using compact devices that may work with renewable energy [4, 5]. In addition, in recent years the electrolysis of water-alcohol mixtures (also called electrochemical reforming or electro-reforming) is emerging as an alternative technique [6] to the electrolysis of water alone due to the lower energy consumption, i.e., around 50% energy saving, since part of the energy is provided by an organic molecule [3, 7, 8].

As a consequence of the above, the electrochemical reforming of alcohols has gained increasing attention in the last few years. Different molecules such as methanol [6, 7, 9-16], ethanol [1, 7, 8, 12, 17-22], bio-ethanol [23] ethylene glycol [3], iso-propanol [12] and glycerol [24-27] have been studied as hydrogen carriers and these have provided interesting results. In these studies, the most effective anodic catalyst is based on highly dispersed Pt-based nanoparticles, e.g., Pt-Ru or Pt-Sn supported on carbon [28-30]. However, due to the lower cost of Sn when compared to Ru, Pt-Sn anodic catalysts are preferred for the electrochemical reforming of alcohols [31, 32]. In particular, an optimal Pt-Sn mass ratio (ca. 3:1), synthesized by the polyol reduction method, was found to be suitable for this purpose due to its higher stability and a lower energy requirement for hydrogen production [8].

The electro-catalytic performance of Pt-based nanoparticles supported on carbon materials depends on both the properties of the support and the corresponding metal-

support interaction. Therefore, for PEM cell applications, previous studies have been focused on commercial Pt-based catalysts supported on Carbon Vulcan XC-72, due to its excellent properties as an anodic support, i.e., high surface area, electrical conductivity and mesoporous structure. However, metal-support interactions can be improved by surface modification of the support. Hence, in the last few decades carbon nanofibers and other related carbon-derived materials, such as graphene flakes, graphene sheets or expanded graphene oxide, have received increased attention due to their distinct structure and characteristics, which enable impressive thermal and electrical properties in various areas [33] and have huge potential in fuel cell development [34] and hydrogen storage [35, 36].

The aim of the work described here was to explore for the first time the possible use of different carbon-based materials as suitable alternatives to commercial Carbon Vulcan XC-72 as the anodic support for the electrochemical reforming of ethanol. For this purpose, different anodic catalysts based on Pt-Sn (3:1 mass ratio) supported on functionalized and non-functionalized low-density carbon nanofibers (CNF f-LS and CNF LS), graphite oxide (GrO), expanded graphite oxide (TRGrO), graphene flakes (GF), β-SiC and Carbon Vulcan XC-72 (C Vulcan, used as reference) were synthesized by the $NaBH_4$ reduction method [37]. Physicochemical and electrochemical characterization was carried out in order to identify the best anodic catalyst for the electrochemical reforming of ethanol. Finally, the selected anodic material was used for further development of a Membrane Electrode Assembly (MEA), which was tested in a number of electro-catalytic experiments in a PEM electrolyser configuration to evaluate its activity and stability for the electrochemical reforming of ethanol to produce hydrogen.

2. Experimental

2.1. Synthesis and characterization of the Pt-Sn catalyst powders

The synthesis of Pt-Sn-based anode catalysts on different carbonaceous supports was carried out according to the $NaBH_4$ reduction method [37]. Firstly, a solution of 800 mg of the selected support in 200 mL of deionized water was prepared and stirred for 6 h. Carbon-based materials used as the anodic support were graphite oxide (GrO) [38, 39], functionalized low-density nanofibers (CNF f-LS) [40], expanded graphite oxide (TRGrO) [38] and graphene flakes (GF) [41], all of which were synthesized in our laboratory, and commercially supplied non-functionalized low-density nanofibers (CNF LS, Graphenano S.L.), β-SiC (Sicat Catalyst) and Carbon Vulcan XC-72 (C Vulcan, Fuel Cell Store). Solutions of $H_2PtCl_6 \cdot 6H_2O$ (398.2 mg in 8 mL deionized water) and $SnCl_2 \cdot 2H_2O$ (95.0 mg in 1.9 mL deionized water) were added to the parent support-solution and this was stirred for 12 h. The solvent was evaporated on a rotavapor at 60 ºC (Rotavapor R-210, Buchi Switzerland). The resulting solid product was dried in an oven at 80 ºC for 12 h (Nabertherm). A 0.2 $mol\ L^{-1}$ ~~$mol \cdot L^{-1}$~~ solution of sodium borohydride was added to the solid sample ($NaBH_4$/precursor molar ratio of 10). A catalyst with a 20 wt. % metal loading with Pt-Sn mass ratio of 3:1 was obtained after filtration and washing to neutral pH.

The Pt and Sn metal loadings impregnated on the different carbonaceous powder supports were determined by atomic absorption (AA) spectrophotometry on a SPECTRA 220FS analyser. Prior to the analysis, samples were treated with 2 mL of hydrochloric acid, 3 mL of hydrofluoric acid and 2 mL of hydrogen peroxide. A microwave digestion at 250 ºC was then carried out [42].

The textural properties of the different Pt-Sn catalysts were evaluated using an ASAP 2010 Micromeritics system with N_2 as the sorbate. Prior to the analysis, samples

were outgassed at 180 ºC under vacuum for 8 h. Specific surface area, mesopore size distribution and microporosity were determined using the Braunauer-Emmett-Teller (multi-point BET) [43], Barret-Joyner-Halenda (BJH) [44] and Horvath-Kawazoe [45] methods, respectively.

X-ray diffraction (XRD) analysis was performed to obtain the crystalline structures of Pt-Sn deposited on the catalysts (powder). A PHILIPS PW-1710 diffractometer with Cu-K_α radiation (λ = 1.5404 Å) was used. Diffractograms were recorded between $10^o \leq 2\theta \leq 100^o$ with a step of 0.02º and compared with JCPDS-ICDD references.

Selected synthesized catalysts were also analyzed by transmission electron microscopy (TEM) to obtain the particle size distribution using a JEOL Model JEM-4000EX unit with an accelerating voltage of 400 kW. Samples were prepared by ultrasonic dispersion of each catalyst in acetone and deposition onto a holey carbon-supported grid prior to evaporation. The particle size distribution was based upon 300 particles for each catalyst [46].

Pulse H_2-chemisorption experiments were also carried out using a commercial Micromeritics AutoChem 2950 HP unit (Chemisorption Analyser Micromertics) in order to determine the dispersion percentage and Pt particle size. Samples were loaded into a U-shaped tube and ramped from room temperature to 473 K (5 $K \cdot min^{-1}$). Pulses of H_2 were then applied at 313.15 K every 4 min (in an argon flow of 15 $cm^3 \cdot min^{-1}$, 99.9999%) until equal peaks were obtained.

Acid/base titrations were performed using a TritoLine system (Schott). Samples of 25 mg of each catalyst were mixed with 25 mL of a 0.1 mol L^{-1} ~~mol·L^{-1}~~ NaCl solution. A 0.1 mol L^{-1} ~~mol·L^{-1}~~ NaOH solution was then added dropwise until a pH value of 11 was reached. The titrant (0.01 mL of a 0.1 mol L^{-1} ~~mol·L^{-1}~~ HCl solution) was then dosed

dropwise until the solution was acidified to pH = 3 (pH meter GLP 22, Crison). The initial NaCl solution was used as a blank to compare the rest of the samples [47, 48].

2.2. Preparation and electrochemical characterization of the Pt-Sn anodes

The different synthesized Pt-Sn/X (20 wt. %) powders were deposited by spraying onto carbon paper substrates (Fuel Cell Earth) by depositing a catalyst ink by mixing the catalyst powder with Nafion solution (5 wt. % Sigma Aldrich) and isopropanol (99.9% for HPLC, Sigma Aldrich), as explained elsewhere [7].

The electrochemical active surface area (ECSA) of each Pt-Sn/X (where X represents the different carbonaceous supports) anodic electrode was measured by means of cyclic voltammetry experiments in a three-electrode electrochemical glass cell (half-cell), as explained elsewhere [19]. The apparatus consisted of an Ag/AgCl reference electrode (3 mol L^{-1} ~~mol·L^{-1}~~ KCl, Metrohm®), a counter electrode with a platinum foil (Metrohm®) and a working electrode (in which the different catalysts were placed). ECSA experiments were run in a solution of 0.5 mol L^{-1} ~~mol·L^{-1}~~ sulfuric acid and 200 cycles were performed (from –0.5 to 1.2 V vs. Ag/AgCl) at scan rate of 50 mV·s^{-1}. Equation 1 was used to calculate the ECSA values from the area of the hydrogen desorption peak [49]:

~~$ECSA\ (m^2 \cdot g^{-1}) = \frac{A_{PtSn}}{\nu \cdot C} \cdot \frac{1}{L_e}$~~

$$ECSA\ (m^2 \cdot g^{-1}) = \left(A_{PtSn} / \nu \cdot C\right) \cdot \left(1 / L_e\right) \qquad \textit{(Equation 1)}$$

where A_{PtSn} is the peak area (AV·cm^{-2}), C is the electrical charge, generally associated with a monolayer of the active Pt-Sn adsorption of hydrogen (0.21 mC·cm^{-2} [50]), ν is the scan rate (V·s^{-1}), and L_e the Pt-Sn loading in the catalyst layer (1.5 mg·cm^{-2}). The degradation of the catalyst was also evaluated from the variation of the electrochemical

active surface area value after 200 cycles. Note that prior to all tests, in order to remove the oxygen dissolved in the acidic media, N_2 gas was bubbled through for at least 20 min. Finally, in order to evaluate the activity of the different anodic electrodes towards the ethanol electro-oxidation reaction in acidic media, cyclic voltammetry experiments were performed on aqueous ethanol 0.5 mol L^{-1} ~~mol·L^{-1}~~ and sulfuric acid 0.5 mol L^{-1} ~~mol·L^{-1}~~ solution. In this test, working electrodes of different Pt-Sn/X materials were employed and a standard three-electrode glass cell was used with a platinum foil (Metrohm®) as counter and Ag/AgCl (3 mol L^{-1} ~~mol·L^{-1}~~ KCl, Metrohm®) as reference electrode. In this case, N_2 was bubbled through the electrolyte for at least 20 min prior to the experiments and an N_2 flow was maintained over the electrolyte during the cyclic voltammetry measurements.

2.3. Electrochemical reforming experiments in the PEM electrolysis cell

Electrochemical reforming measurements were carried out in a PEM electrolysis cell described in detail elsewhere [7]. In the PEM electrolysis cell, the Membrane Electrode Assembly (MEA) consisted of a proton exchange membrane (Nafion® 117, Hidrógena S. A.) and two working electrodes (anode and cathode). A commercial Pt supported on Carbon Vulcan XC-72 catalyst (20 wt. % Pt/C, Alfa Aesar) was used as the cathode, while the selected Pt-Sn/CNF LS (20 wt. %) was used as the anode.

A 4 mol L^{-1} ~~mol·L^{-1}~~ ethanol-water solution (1 L, feeding rate of 3 mL·min^{-1}) was fed into the anodic chamber, this concentration was selected as the optimal one according to previous studies [1, 8, 23], and water (1 L, feeding rate of 3 mL·min^{-1}) was fed into the cathodic chamber, using in both cases a peristaltic pump (Pumpdrive 5001, Heidolph). The operation mode was discontinuous, i.e., both outlet streams were recirculated to the feed reservoirs.

Different types of electrochemical measurements were carried out. In the first place, both solutions were preheated to between 30 ºC and 80 ºC and experimental data for linear voltammetry (LV) were recorded with a gradual polarization from 0 to 1.4 V and at a scan rate of 5 $mV \cdot s^{-1}$. Chronopotentiometric experiments were then performed to demonstrate the stability and durability of the system. For this purpose, an experiment with an overall duration of 24 h at 80 ºC was carried out. The experiment involved four cycles of 6 h duration each at different currents (the first set at 0.1 A and 0.2 A, and a second set at 0.2 A and 0.1 A). In addition, in order to demonstrate the possible regeneration of the system, different electrochemical regeneration treatments were performed between different chronopotentiometry experiments at 0.2 A and 80 ºC. The two different regeneration steps involved leaving the cell for 10 min under either open circuit conditions (OCV) or polarization at 1.7 V. The selected regeneration treatment was also explored by eleven consecutive cycles in a mild-term experiment of 450 min.

Finally, electrochemical impedance spectroscopy (EIS) studies were carried out, prior- and post-stability tests, to obtain information about the behavior of the MEA (ohmic resistance and charge transfer resistance). This experiment was performed using the impedance module of the Ivium potentiostat/galvanostat at a potential of 0.7 V. The cell impedance spectra were recorded over a frequency range from 10 kHz to 10 mHz with a potential amplitude of 10 mV at 80 ºC. All of the electrochemical measurements performed in this study were carried out using a Vertex 5A.DC, a potentiostat/galvanostat (Electrochemical Analyzer, Ivium Technologies) controlled by research electrochemistry software.

3. Results and discussion

3.1. Physicochemical Characterization

Physicochemical characterization of the synthesized catalysts was achieved by means of atomic absorption spectrometry (AA), X-ray diffraction (XRD), transmission electron microscopy (TEM) and nitrogen adsorption-desorption measurements, as summarized in Table 1.

Table 1. Summary of physicochemical anodic catalyst characterization

CATALYSTS		% Metal		BET Area ($m^2 \cdot g^{-1}$)	
		% Pt	% Sn	Support	Catalyst
PtSn/	C Vulcan	14.2	4.2	229.6	196.6
	CNF LS	13.4	4.7	131.9	109.6
	CNF f-LS	16.1	5.1	126.3	113.8
	TRGrO	14.1	5.3	104.2	97.0
	GF	14.5	4.6	26.7	19.2
	GrO	16.0	4.7	20.3	10.2
	β-SiC	15.1	4.9	26.3	21.2

It can be seen from the results in Table 1 that the atomic absorption (AA) spectrophotometry results corresponded, with a little variation, to the intended Pt-Sn total loading (around to 20 wt. %), with the specified mass ratio of 3:1 (Pt-Sn) obtained in all samples. The specific surface areas of different carbonaceous supports and the corresponding catalysts after Pt-Sn addition are also shown in Table 1. The BET surface area values collected in Table 1 are consistent with those found in the literature for the different materials: Carbon Vulcan XC-72 [51, 52], β-SiC [50], GF [53] and CNF LS [52]. Moreover, it can also be observed that the specific surface areas of the different catalysts were smaller than those of the initial support materials due to partial blocking of the support pores by Pt-Sn particles after metal precursor impregnation [54]. Pt-Sn catalysts supported on Carbon Vulcan XC-72 (for comparative purposes), CNF LS, CNF f-LS and TRGrO presented a combination of type I and IV isotherms (not shown here)

with an H1 adsorption-desorption hysteresis loop, which is typical of mesoporous carbonaceous materials [55]. Pt-Sn catalysts supported on β-SiC, GrO and GF were low porosity materials, with a lower surface area than the other carbonaceous materials. It is known that the support plays a key role in the dispersion of the active phase particles [33]. Therefore, a support with a higher BET surface area is desirable since it would favor a better dispersion of the catalyst particles [56] and avoid agglomeration during the synthesis, thus enhancing the catalytic/electro-catalytic activity [57]. In this sense, of the proposed catalysts, Pt-Sn deposited on Carbon Vulcan XC-72, CNF LS and CNF f-LS showed higher specific surface area values than TRGrO, GF, GrO or β-SiC. These differences can be attributed to the different structure of each carbon material. For example, Carbon Vulcan XC-72 has a reduced pore size and its structure contains micropores into which nanoparticles can sink, thus reducing the number of three-phase boundary active sites [58]. On the other hand, CNFs can present a high or low specific area depending on the method of synthesis, but they are characterized by highly ordered graphene sheets that show high electrical conductivity and chemical stability [58]. However, GrO consists of wrinkled graphene layers with a high number of defects, which in turn leads to lower electrical conduction [59, 60]. In agreement with the above, the highest specific surface area corresponds to Pt-Sn supported on the Carbon Vulcan XC-72 commercial support with a more homogeneous pore distribution, which was used as a reference material for comparative purposes. Pt-Sn catalysts supported on CNF LS and CNF f-LS (in comparison with the catalyst supported on the commercial Carbon Vulcan XC-72) would also be promising candidates to provide suitable electro-catalytic activity [50] since they have the appropriate specific surface area, which may be directly related to the electrochemical activity of the catalyst [56, 61].

The XRD results for Pt-Sn anodic catalysts on different carbonaceous supports (Pt-Sn/X, where X is the different carbonaceous material) are presented in Figure 1. The main peak for crystalline platinum can be clearly observed and this is consistent with the active phase being deposited correctly on the different supports and confirms that the synthesis method was suitable [50].

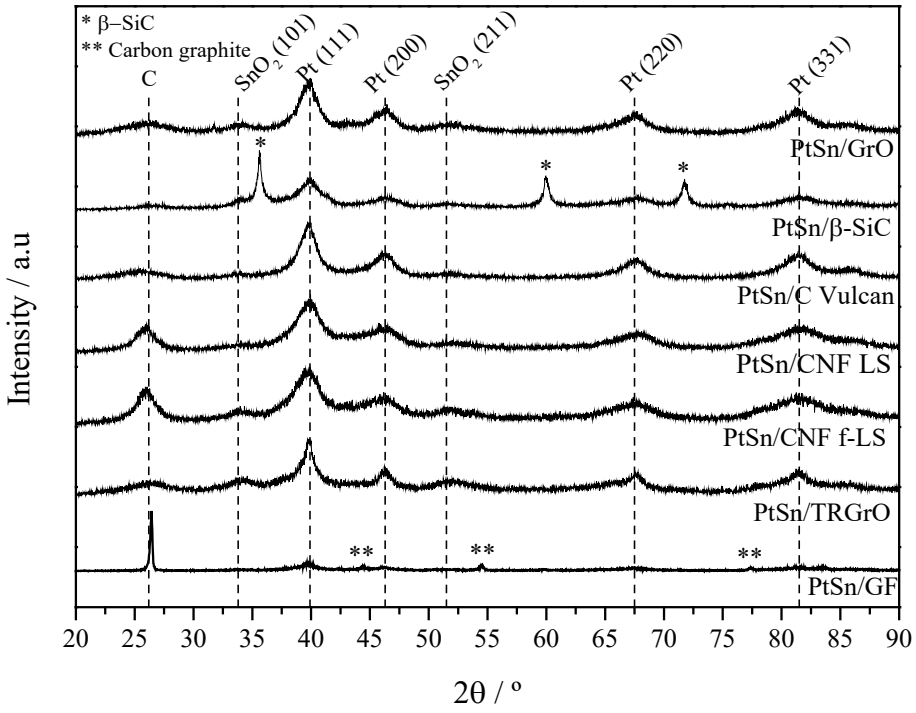

Figure 1. XRD patterns of different Pt-Sn/X anodic catalysts.

Peaks at 2θ values of around 40, 46, 68 and 81º corresponded to Pt fcc reflections (111), (200), (220) and (331), respectively [7, 62, 63]. Peaks at 2θ values of around 34º and 54º correspond to SnO_2 tetragonal reflections (101) and (211), respectively [64]. The XRD patterns also contain a peak at a 2θ values around 25º and this corresponds to the hexagonal structure of the C in each support [62]. It is also worth noting that the intensity of the graphite-related peak in all carbonaceous supports described here is significantly

higher than that of the commercial Carbon Vulcan XC-72. This finding is due to the different graphitization degrees of the different carbonaceous supports [52].

TEM measurements ~~was~~ were performed on the catalyst with the highest active surface area, namely Pt-Sn/CNF LS, since this catalyst was considered to be the most promising for the electrochemical reforming of ethanol. Pt-Sn/C Vulcan was also analyzed for comparative purposes. In order to corroborate the physicochemical characterization, the TEM micrographs and particle size distributions of the Pt-Sn/C Vulcan and Pt-Sn/CNF LS catalysts are provided in Figure 2. Note that average Pt particle size was calculated by considering more than 400 particles from the TEM analysis.

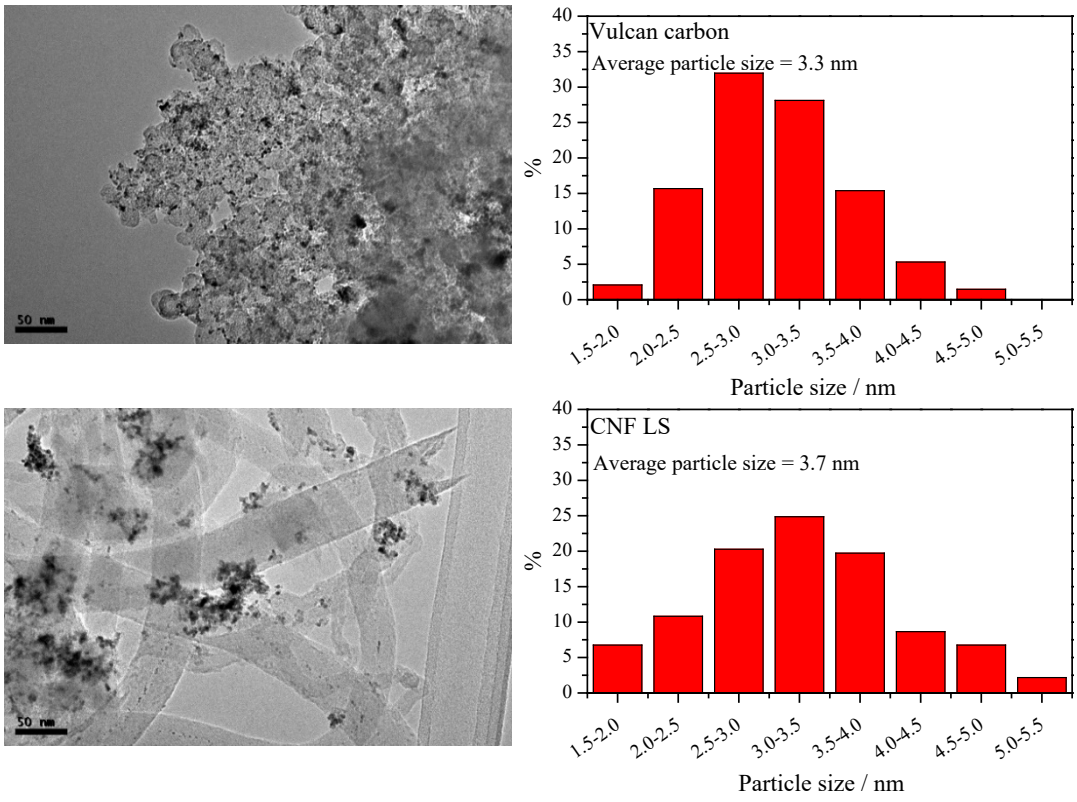

Figure 2. TEM images of Pt-Sn/C Vulcan and Pt-Sn/CNF LS catalysts.

It is known that a small particle size probably leads to better electrochemical behavior due to the increase in the electrochemical surface area of the catalyst [62]. However, there is very little difference in the Pt particle sizes values found for the two supports (around 3.5 nm) and this demonstrates that the borohydride reduction method was suitable for the synthesis of catalysts with a nanometre size [65]. Particle size and the dispersion percentage were also calculated for both anodic catalysts using the pulse H_2-chemisorption technique. It was confirmed that there were no significant differences in either case (31.2% and 26.3% dispersion, 3.2 nm and 3.8 nm Pt particle size for Pt-Sn/C Vulcan and Pt-Sn/CNF LS, respectively) and these results are in excellent agreement with the TEM analysis [66]. In addition, an acid-base titration experiment was carried out in order to determine the different behaviors of the Pt-Sn/C Vulcan and Pt-Sn/CNF LS catalysts. The Pt-Sn catalyst supported on Carbon Vulcan XC-72 presented slightly lower basicity (30.0 $cm^3 \cdot g^{-1}$) in comparison to the Pt-Sn catalyst supported on CNF LS (33.2 $cm^3 \cdot g^{-1}$).

3.2. Electro-catalytic experiments in a three-electrode glass cell

The electrochemical active surface area (ECSA) of each synthetized catalyst was evaluated by cyclic voltammetry in 0.5 mol L^{-1} ~~mol·L^{-1}~~ sulfuric acid at a scan rate of 50 $mV \cdot s^{-1}$ at room temperature. From the results in Table 2 it can be observed that Pt-Sn supported on Carbon Vulcan XC-72, CNF f-LS and, especially, CNF LS presented the highest ECSA values and lowest variation between them in cycles 1 and 200, which indicates a lower degree of degradation of these materials [67]. (As a representative example, the 1st and 200th cycles for the Pt-Sn supported on CNF-LS and C Vulcan are shown in Figure S1 in the Supporting Information).

Table 2. ECSA values for the different Pt-Sn/X anodic catalysts.

CATALYSTS		ECSA ($m^2 \cdot g^{-1}$)		
		Cycle 1	Cycle 200	% degradation
PtSn/	C Vulcan	30.5	25.3	17.2
	CNF LS	32.5	28.4	12.4
	CNF f-LS	31.5	27.7	11.0
	TRGrO	-	-	-
	GF	28.2	24.5	13.0
	GrO	4.3	3.6	16.3
	β-SiC	1.3	0.6	55.5

The Pt-Sn supported on TRGrO, GrO and β-SiC presented much lower ECSA values and this is likely to lead to lower electro-catalytic activity [49]. This difference can be attributed to the combination of low surface area and lower electrical conductivity of these carbonaceous supports when compared with the other materials [68, 69].

The results obtained in the cyclic voltammetry experiments are provided in Figure 3. A scan of 25 cycles was carried out (scan 25 shown in Figure 3a) and the completed CV for Pt-Sn/CNF LS, by varying the potential between –0.2 V and 1.0 V vs. Ag/AgCl, is shown in Figure 3b. These experiments were performed using a 0.5 mol L^{-1} ~~mol·L^{-1}~~ ethanol and 0.5 mol L^{-1} ~~mol·L^{-1}~~ H_2SO_4 solution at a scan rate 20 $mV \cdot s^{-1}$ at 80 ºC. Furthermore, some electrochemical characterization was carried out in a Rotating Disk Electrode (RDE) in order to corroborate the stability of the electrode under the reaction conditions (not shown here; see Supporting Information, Figure S2).

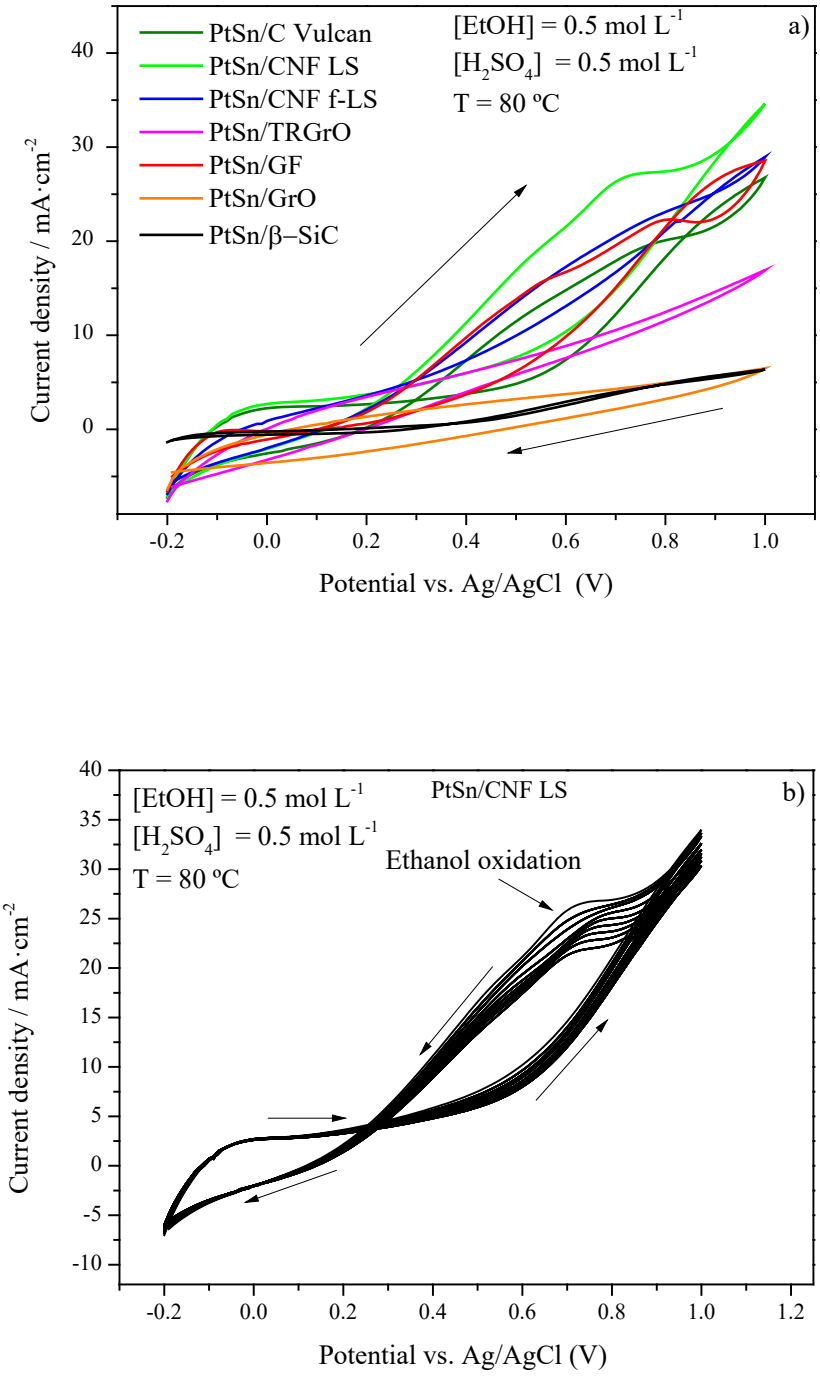

Figure 3. Cyclic Voltammetry results for catalysts a) Pt-Sn/X and b) Complete CV for Pt-Sn/CNF LS catalyst (ethanol 0.5 mol L^{-1} ~~mol·L^{-1}~~ + H_2SO_4 0.5 mol L^{-1} ~~mol·L^{-1}~~ at 80 ºC at the scan rate 20 $mV \cdot s^{-1}$).

As one would expect, it can be observed that the shapes of the curves are characteristic of the ethanol electro-oxidation reaction [8]. In addition, hysteresis features in the current values during the backward scans were higher than the current values in the forward scans and these can be attributed to changes in the catalyst surface. During the backward scan, after reaching the highest potential values, there were changes in the platinum oxidation state that could affect the absorption of the alcohol and lead to a higher electro-catalytic rate [12].

It was observed that, of the different catalysts investigated, Pt-Sn/CNF LS showed the highest electro-catalytic activity for the ethanol electro-oxidation reaction. This finding can be attributed to a combination of physicochemical and electrochemical properties such as high surface area (which enables good dispersion of the Pt-Sn nanoparticles), a slightly higher basicity than Carbon Vulcan XC-72 (which promotes conductivity) and a high ECSA value with low electrochemical degradation (which provides a better electronic pathway in comparison with other carbon-supported materials) [58, 70, 71]. On the other hand, Pt-Sn/CNF f-LS and Pt-Sn/GF were also found to be suitable candidates for ethanol electro-oxidation and this is again in good agreement with the high ECSA values and low degradation shown by these materials. Conversely, catalysts Pt-Sn/GrO, Pt-Sn/TRGrO and Pt-Sn/β-SiC presented lower electro-catalytic activity and this could be attributed to the lower surface area and ECSA values, which are directly related to the nature of these materials. On the basis of these results, Pt-Sn/CNF LS was selected as the best anodic catalyst for the subsequent preparation of a Membrane Electrode Assembly (MEA) (as described in the experimental section) to be tested in a PEM cell for the electrochemical reforming of ethanol.

3.3. Electro-catalytic experiments in the PEM electrolysis cell

Linear voltammetry experiments were performed at different temperatures (ranging from 30 to 80 ºC). A 4 mol L^{-1} ~~mol·L^{-1}~~ ethanol solution was fed into the anode compartment as this was reported to be the optimal concentration in previous studies carried out by our group [1, 8, 23]. The polarization curves obtained on using Pt-Sn/CNF LS and commercial Pt/C as anodic and cathodic catalyst, respectively, at a scan rate of 5 $mV \cdot s^{-1}$ at 30, 50, 70 and 80 ºC are presented in Figure 4.

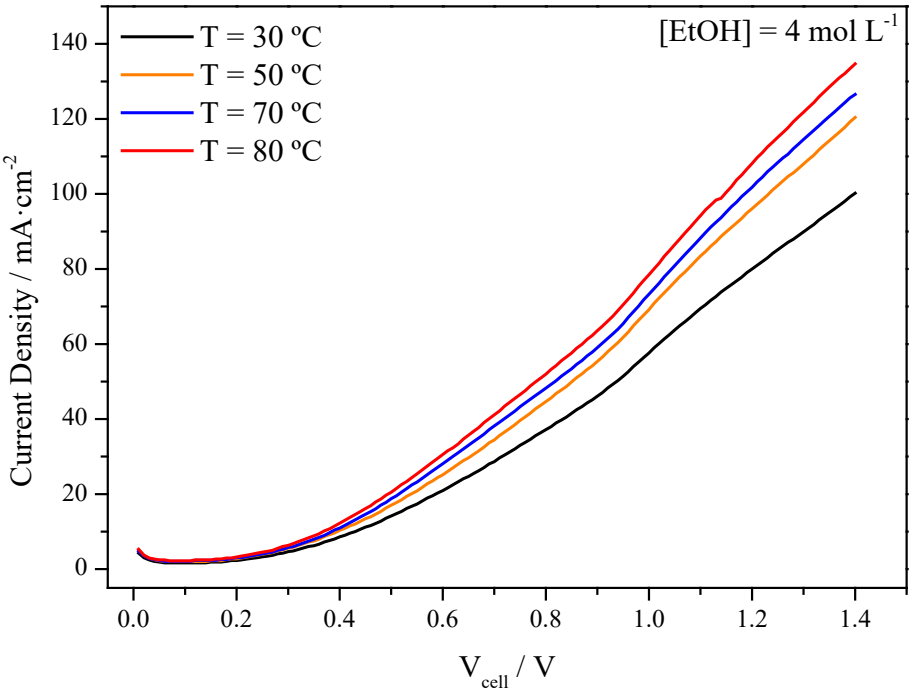

Figure 4. Influence of the temperature on the polarization curves for a MEA based on Pt-Sn/CNF LS as the anodic catalyst (ethanol 4 mol L^{-1} ~~mol·L^{-1}~~ anode solution at temperature of 30, 50, 70 and 80 ºC at a scan rate 5 $mV \cdot s^{-1}$).

It can be seen that an increase in the temperature of the cell led to an increase in the current density due to the improvement in both the kinetics and ionic conductivity of the membrane, a finding in good agreement with the results of previous studies [1, 23,

24]. Note that there is no evidence of mass transfer limitations at any temperature over the explored potential range [23]. Furthermore, at 80 $mA \cdot cm^{-2}$ an energy requirement reduction from 32 $kWh \cdot kg_{H2}^{-1}$ to 27 $kWh \cdot kg_{H2}^{-1}$ can be obtained by increasing the temperature from 30 to 80 ºC. Therefore, due to the significant improvement in the linear voltammetry at 80 ºC and, consequently, H_2 production rates at a lower potential values, this temperature was selected as the working temperature for the subsequent experiments. Similar findings were reported in in previous studies [3, 7, 8, 19, 23].

The next step was to verify the stability of the system and the viability for practical application in a mild-term electrochemical reforming experiment. With this aim in mind, chronopotentiometric experiments were performed with different cycles, i.e., increasing and then decreasing the applied current (between 0.1 A and 0.2 A) as shown in Figure 5. Experiments were run under the conditions selected above (4 mol L^{-1} ~~mol·L^{-1}~~ ethanol solution and 80 ºC) for a total duration of 24 h for 4 consecutive cycles of 6 h of duration each.

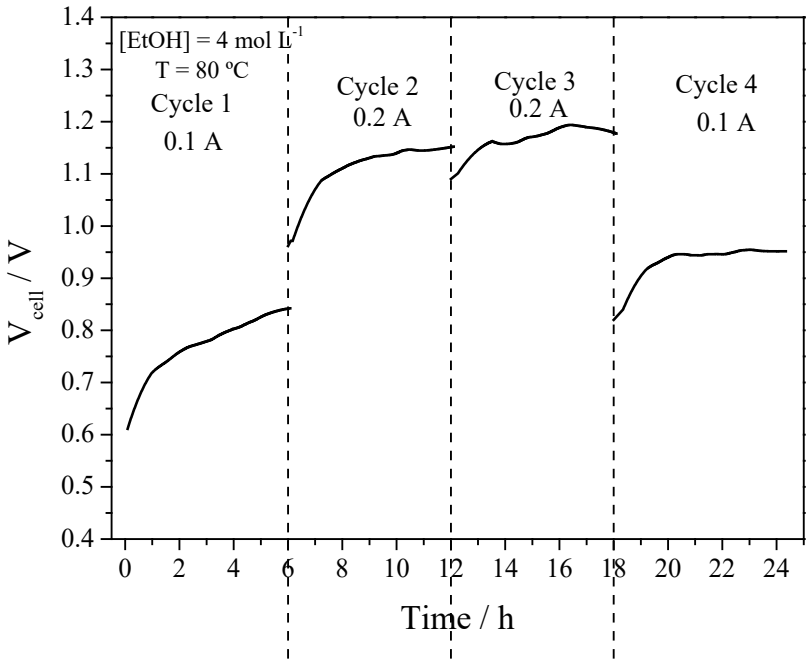

Figure 5. Chronopotentiometry experiment for an MEA based on a Pt-Sn/CNF LS anodic catalyst (constant current density of 0.1 A and 0.2 A with an ethanol 4 mol L^{-1} ~~mol·L^{-1}~~ anode solution at 80 ºC).

The stability was analysed by measuring the variation of potential with time during the galvanostatic polarization experiments. Initially a continuous increase in the potential values with time can be observed during each galvanostatic experiment. The increase in the potential values at the beginning of each experiment can be attributed to the adsorption of intermediate reaction species (e.g., acetaldehyde) on the anodic catalyst during the ethanol electro-oxidation reaction [7, 19]. The system then seems to achieve an almost steady-state value at around four working hours. In the case of cycles 2 and 3, which were performed at the same current, the system showed a slight regeneration during the open circuit conditions carried out between the cycles (around 5 seconds duration). This observation seems to indicate that the system can be partially regenerated due to the partial removal of the intermediate adsorbed species during the open circuit condition

step. However, a continuous and irreversible degradation could be observed with time since higher potential values in cycle 4 were obtained when compared to cycle 1, which was performed under the same current. Stability and regeneration studies were carried out in order to elucidate the possible degradation and regeneration mechanisms and extended performance.

3.4. Extended performance stability and regeneration study in the PEM electrolysis cell

In order to study the possible regeneration of the MEA during the electrochemical reforming of ethanol, two series of experiments with two different regeneration treatments were conducted (see Figure 6). Cycles of 0.2 A (30 min) were alternated with Open Circuit Voltage (OCV) or the application of 1.7 V as regeneration periods (10 min) and these were carried out three times.

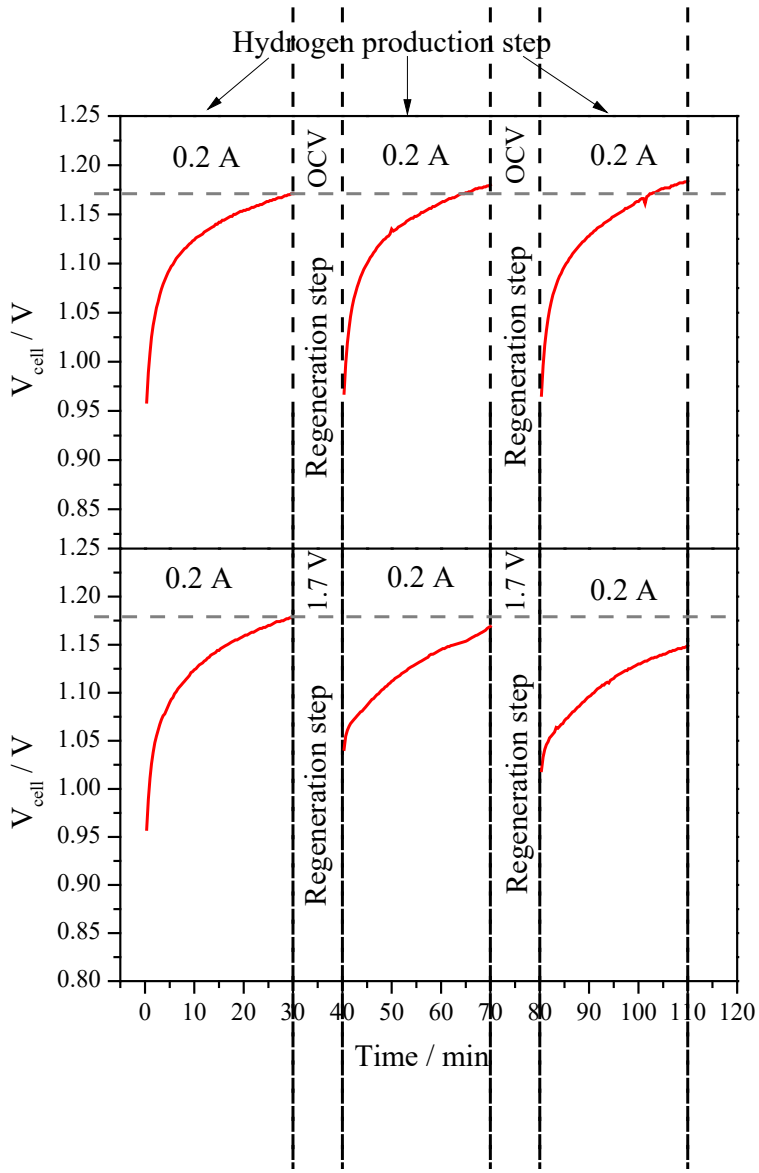

Figure 6. Variation of the total voltage of the cell vs. time under the application of different regeneration cycles for an MEA based on a Pt-Sn/CNF LS anodic catalyst (ethanol 4 mol L^{-1} ~~mol·L^{-1}~~ anode solution at 80 ºC, regeneration cycles of OCV and 1.7 V).

It can be observed that both regeneration treatments seem in principle to regenerate partially the anodic catalyst surface from adsorbed carbonaceous species, since the potential values at each galvanostatic polarization followed a similar trend. However, the second regeneration treatment involving the application of 1.7 V allowed a decrease

in the potential values in the subsequent regeneration steps. This second regeneration treatment is probably more effective for the removal of carbonaceous adsorbed molecules, which block active anodic sites. The application of 1.7 V may have led to the electrochemical oxidation of the intermediate adsorbed molecules. In addition, at 1.7 V the evolution of O_2 due to the water splitting reaction starts to take place and this allows further oxidation of these intermediate reaction species. Therefore, the electrochemical oxidation of intermediate adsorbed species in the second regeneration procedure seems to be a more effective approach than simply leaving the system under open circuit conditions.

The results for the second regeneration procedure over a longer period of time are shown in Figure 7a, whereas the average potential values registered during the regeneration procedure are shown in Figure 7b. The experiment consisted of 11 cycles of hydrogen production during 30 min under a galvanostatic polarization of 0.2 A, and 10 regeneration cycles of 10 min by applying a potential of 1.7 V.

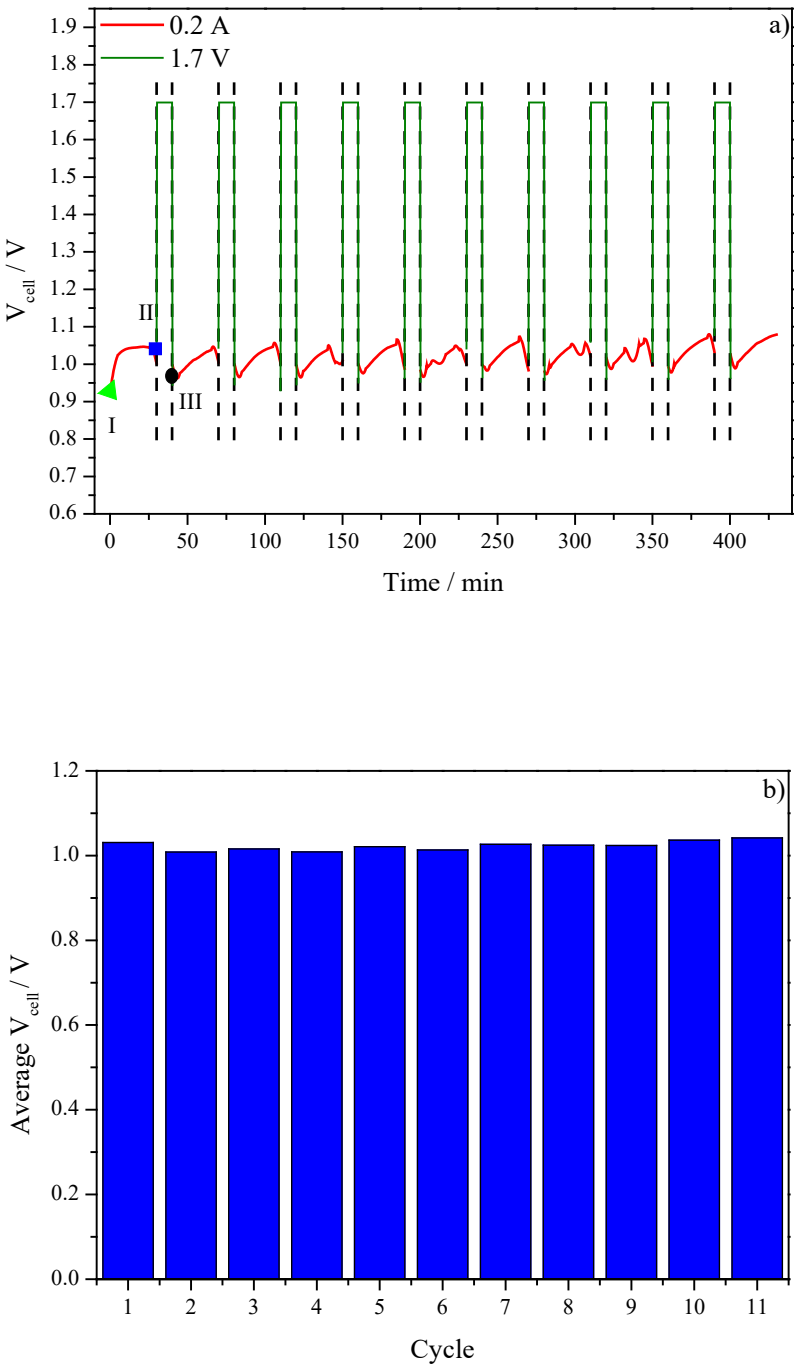

Figure 7. a) Variation of the total voltage of the cell vs. time under the application of different regeneration cycles for an MEA based on a Pt-Sn/CNF LS anodic catalyst (ethanol 4 mol L^{-1} ~~mol·L^{-1}~~ anode solution at 80 ºC, regeneration cycles of 1.7 V) and b) average voltage of the cell during the different regeneration cycles.

It can be observed that the system could, in principle, be regenerated a number of times throughout the different cycles. The presence of some potential peaks during the galvanostatic applications in the hydrogen production steps could also be attributed to the electro-oxidation of accumulated intermediate species adsorbed on the anodic catalyst during the electro-reforming [1]. Similar average potential values were obtained under the different galvanostatic polarizations of 0.2 A, which demonstrates the reproducible behavior of the MEA during different polarizations as well as the advantage of adding a regeneration period between the different current application stages for longer working times. Furthermore, as shown in Figure 7b, the average potential reached in the different cycles does not change, which means that the MEA system remains stable, which is in good agreement with previous works [7, 8, 19].

Finally, electrochemical impedance spectroscopy (EIS) experiments were carried out before and after the chronopotentiometric tests and also after the regeneration experiments, marked as *States I, II* and *III* in Figure 7a. The corresponding Nyquist plots obtained after each experiment are shown in Figure 8. EIS experiments were performed using a constant potential of 0.7 V and under the application of frequencies from 10 kHz to 10 mHz with a potential amplitude of 10 mV.

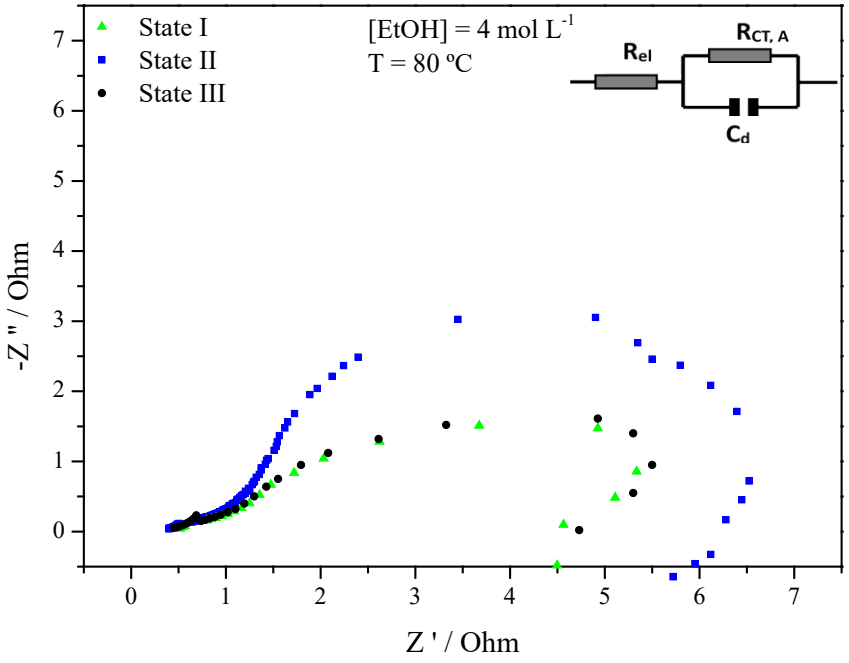

Figure 8. Impedance spectra of the MEA at a constant potential of 0.7 V before (*State I*) and after (*State II*) the performance of chronopotentiometry (State II) and regeneration experiments (*State III*) for Pt-Sn/CNF LS catalyst (ethanol 4 mol L^{-1} ~~mol·L^{-1}~~ anode solution at 80 ºC).

~~In agreement with previous studies with similar MEAs [8], two semicircles were observed in the Nyquist plots of the EIS, which can be related to the cathodic (first semicircle at higher frequencies) and anodic reactions (second semicircle at lower frequencies).~~ In agreement with the results of previous studies on similar MEAs [23], two semicircles were observed in the Nyquist plots of the EIS and these can be related to the different main resistances present in the system. From these experiments, two main resistances of the system were calculated: the ohmic resistance associated mainly with the resistance of the membrane, catalyst layer, gas diffusion layer and bipolar plates (first cut with the real axis, R_s) [72], and the second one, related to the charge transfer resistance (R_{TC}) (due to the absence of mass transfer limitations) [73]. In addition, it is well known

that for the electrochemical reforming of ethanol with this kind of MEA, the anodic overpotential is the main charge transfer resistance, since a negligible cathodic overpotential contribution on a similar configuration has been identified [12]. The resistance values calculated from the previous EIS experiments are provided in Table 3.

Table 3. Summary of the ohmic resistance and combined mass and charge transfer resistances calculated from the Nyquist plot of the impedance spectra.

	R_s / Ohm	R_{TC} / Ohm
State I	0.397	4.167
State II	0.405	5.714
State III	0.407	4.323

It can be observed that the resistance of the membrane increases slightly during the experiments, probably due to a slight decrease in the ionic conductivity with operation time of the membrane. On the other hand, an increase in the charge transfer resistance can be observed and this is associated with the anodic charge transfer reaction for *State II* vs. *State I*. As one would expect, a higher anodic resistance value implied a lower electro-catalytic activity. This is consistent with the results discussed above and can be attributed to the physicochemical blocking of the anode by intermediate adsorption species [74]. Finally, it can be observed that after the regeneration treatment on *State III,* the anodic resistance decreased again due to the removal of the intermediate adsorbed molecules by electro-oxidation. This process allows partial regeneration of the anodic catalyst, thus increasing again the anode kinetics for the ethanol electro-oxidation reaction and leading to almost identical EIS spectra for *State II* and *State III*. This finding is consistent with the average potential values shown in Figure 7b and demonstrates the possibility of regenerating the anodic catalyst a number of times in view of the practical application of the system.

In conclusion, the synthetized Pt-Sn/CNF LS is a novel anodic catalyst suitable for the electrochemical reforming of ethanol in acidic media due to its physicochemical characteristics and electro-catalytic behavior. In addition, a regeneration process can be carried out in view of the practical application of the electrochemical reforming unit for hydrogen production.

4. Conclusions

~~Platinum-tin catalysts deposited on different carbon-based supports have been prepared, characterized and tested on the electrochemical reforming of ethanol for hydrogen production. The following conclusions have been obtained from this study:~~

~~- Functionalized and non-functionalized low-density nanofibers and graphene flakes seems to be an alternative to commercial Carbon Vulcan XC-72 used as anodic catalyst support for hydrogen production via electrochemical reforming of ethanol.~~

~~-Among the different explored anodic catalyst, Pt-Sn supported on non-functionalized low-density nanofibers (CNF-LS) showed the highest ethanol electro-oxidation activity. It was attributed to a combination of physicochemical and electrochemical properties related to the structure of this support, such as high surface area, which results in good dispersion of the catalyst nanoparticles, high basicity and a high ECSA value with low electrochemical degradation.~~

~~- Pt-Sn supported on non-functionalized low-density nanofibers was were chosen for the development of a Membrane Electrode Assembly (MEA). A high electrochemical reforming activity was obtained (120 mA·cm^{-2} at 1.4 V and 80 ºC) for hydrogen production which led to energy consumption values below 30 kWh·kg$_{H_2}^{-1}$.~~

~~-A number of mild term electrochemical reforming tests were performed in order to demonstrate the durability of the MEA (stability of the anodic catalyst and the~~

~~membrane). The observed deactivation vs. time was attributed to the adsorption of intermediate electro-oxidation products on the anodic catalyst, which increased the anodic charge transfer resistance. The application of regenerating periods under a polarization of 1.7 V allows to completely regenerate the MEA, via the electro-oxidation of these intermediates molecules.~~

Platinum-tin catalysts deposited on different carbon-based supports have been prepared, characterized and tested in the electrochemical reforming of ethanol for hydrogen production. The best alternatives to the commercial Carbon Vulcan XC-72 seems to be functionalized and non-functionalized low-density nanofibers and graphene flakes, which were used as anodic catalyst supports for hydrogen production by the electrochemical reforming of ethanol.

Among them, Pt-Sn supported on non-functionalized low-density nanofibers (CNF LS) showed the highest ethanol electro-oxidation activity. This result was attributed to a combination of physicochemical and electrochemical properties related to the structure of this support, such as high BET surface area, which results in good dispersion of the catalyst nanoparticles, high basicity and a high ECSA value with low electrochemical degradation.

For these reasons, Pt-Sn supported on non-functionalized low-density nanofibers ~~was~~ were chosen for the development of a Membrane Electrode Assembly (MEA). This system presents energy consumption values below 30 $kWh \cdot kg_{H_2}^{-1}$ for hydrogen production in the electrochemical reforming of ethanol, with an electrochemical reforming activity of 120 $mA \cdot cm^{-2}$ at 1.4 V and 80 ºC.

In order to demonstrate the durability of the MEA (stability of the anodic catalyst and the membrane), a number of mild-term electrochemical reforming tests were

performed. The observed deactivation over time was attributed to the adsorption of intermediate electro-oxidation products on the anodic catalyst, which increased the anodic charge transfer resistance. The application of regenerating periods under a polarization of 1.7 V allowed the complete regeneration of the MEA through the electro-oxidation of these intermediate molecules.

Acknowledgments

We gratefully acknowledge the Spanish Ministry of Economy and Competiveness (project CTQ2016-75491-R) for financial support. A. B. Calcerrada would like to thank the Junta de Comunidades de Castilla-La Mancha (JCCM) and the European Social Fund for financial support.

REFERENCES

[1] Caravaca A, Sapountzi FM, De Lucas-Consuegra A, Molina-Mora C, Dorado F, Valverde JL. Electrochemical reforming of ethanol-water solutions for pure H 2 production in a PEM electrolysis cell. Int J Hydrog Energ, 2012;37:9504-13.

[2] Sasikumar G, Muthumeenal A, Pethaiah SS, Nachiappan N, Balaji R. Aqueous methanol eletrolysis using proton conducting membrane for hydrogen production. Int J Hydrog Energ, 2008;33:5905-10.

[3] de Lucas-Consuegra A, Calcerrada AB, de la Osa AR, Valverde JL. Electrochemical reforming of ethylene glycol. Influence of the operation parameters, simulation and its optimization. Fuel Process Technol, 2014;127:13-9.

[4] Papazisi KM, Siokou A, Balomenou S, Tsiplakides D. Preparation and characterization of IrxPt1−xO2 anode electrocatalysts for the oxygen evolution reaction. Int J Hydrog Energ, 2012;37:16642-8.

[5] Carmo M, Fritz DL, Mergel J, Stolten D. A comprehensive review on PEM water electrolysis. Int J Hydrog Energ, 2013;38:4901-34.

[6] Lamy C, Guenot B, Cretin M, Pourcelly G. A kinetics analysis of methanol oxidation under electrolysis/fuel cell working conditions. In: Atanassov P, Minteer SD, Shao M, editors. Symposium on Electrocatalysis 7 - 227th ECS Meeting. 29 ed: Electrochemical Society Inc.; 2015. p. 1-12.

[7] de la Osa AR, Calcerrada AB, Valverde JL, Baranova EA, de Lucas-Consuegra A. Electrochemical reforming of alcohols on nanostructured platinum-tin catalyst-electrodes. Appl Catal B-Environ, 2015;179:276-84.

[8] Calcerrada AB, de la Osa AR, Dole HAE, Dorado F, Baranova EA, de Lucas-Consuegra A. Stability Testing of Pt x Sn1 − x /C Anodic Catalyst for Renewable Hydrogen Production Via Electrochemical Reforming of Ethanol. Electrocatalysis-US, 2017.

[9] González-Cobos J, López-Pedrajas D, Ruiz-López E, Valverde JL, de Lucas-Consuegra A. Applications of the electrochemical promotion of catalysis in methanol conversion processes. Top Catal, 2015;58:1290-302.

[10] De Lucas-Consuegra A, González-Cobos J, Gacia-Rodriguez Y, Endrino JL, Valverde JL. Electrochemical activation of the catalytic methanol reforming reaction for H 2 production. Electrochem Commun, 2012;19:55-8.

[11] Naga Mahesh K, Balaji R, Dhathathreyan KS. Palladium nanoparticles as hydrogen evolution reaction (HER) electrocatalyst in electrochemical methanol reformer. Int J Hydrog Energ, 2016;41:46-51.
[12] Sapountzi FM, Tsampas MN, Fredriksson HOA, Gracia JM, Niemantsverdriet JW. Hydrogen from electrochemical reforming of C1–C3 alcohols using proton conducting membranes. Int J Hydrog Energ, 2017;42:10762-74.
[13] Cloutier CR, Wilkinson DP. Electrolytic production of hydrogen from aqueous acidic methanol solutions. Int J Hydrog Energ, 2010;35:3967-84.
[14] Pham AT, Baba T, Shudo T. Efficient hydrogen production from aqueous methanol in a PEM electrolyzer with porous metal flow field: Influence of change in grain diameter and material of porous metal flow field. Int J Hydrog Energ, 2013;38:9945-53.
[15] Uhm S, Jeon H, Kim TJ, Lee J. Clean hydrogen production from methanol-water solutions via power-saved electrolytic reforming process. J Power Sources, 2012;198:218-22.
[16] Antolini E. Carbon supports for low-temperature fuel cell catalysts. Appl Catal B-Environ, 2009;88:1-24.
[17] Lamy C, Jaubert T, Baranton S, Coutanceau C. Clean hydrogen generation through the electrocatalytic oxidation of ethanol in a Proton Exchange Membrane Electrolysis Cell (PEMEC): Effect of the nature and structure of the catalytic anode. J Power Sources, 2014;245:927-36.
[18] Chen YX, Lavacchi A, Miller HA, Bevilacqua M, Filippi J, Innocenti M, et al. Nanotechnology makes biomass electrolysis more energy efficient than water electrolysis. Nat Commun, 2014;5.
[19] de Lucas-Consuegra A, de la Osa AR, Calcerrada AB, Linares JJ, Horwat D. A novel sputtered Pd mesh architecture as an advanced electrocatalyst for highly efficient hydrogen production. J Power Sources, 2016;321:248-56.
[20] Jablonski A, Lewera A. Electrocatalytic oxidation of ethanol on Pt, Pt-Ru and Pt-Sn nanoparticles in polymer electrolyte membrane fuel cell-Role of oxygen permeation. Appl Catal B-Environ, 2012;115-116:25-30.
[21] Coutanceau C, Baranton S. Electrochemical conversion of alcohols for hydrogen production: a short overview. Wiley Interdisciplinary Reviews: Energy and Environment. 2016;5:388-400.

[22] Calcerrada AB, de la Osa AR, Llanos J, Dorado F, de Lucas-Consuegra A. Hydrogen from electrochemical reforming of ethanol assisted by sulfuric acid addition. Appl Catal B-Environ, 2018;231:310-6.
[23] Caravaca A, De Lucas-Consuegra A, Calcerrada AB, Lobato J, Valverde JL, Dorado F. From biomass to pure hydrogen: Electrochemical reforming of bio-ethanol in a PEM electrolyser. Appl Catal B-Environ, 2013;134-135:302-9.
[24] De Paula J, Nascimento D, Linares JJ. Electrochemical reforming of glycerol in alkaline PBI-based PEM reactor for hydrogen production. Chemical Engineering Transactions 2014. p. 205-10.
[25] Marshall AT, Haverkamp RG. Production of hydrogen by the electrochemical reforming of glycerol–water solutions in a PEM electrolysis cell. Int J Hydrog Energ, 2008;33:4649-54.
[26] de Paula J, Nascimento D, Linares J. Influence of the anolyte feed conditions on the performance of an alkaline glycerol electroreforming reactor. J Appl Electrochem, 2015;45:689-700.
[27] Kongjao S, Damronglerd S, Hunsom M. Electrochemical reforming of an acidic aqueous glycerol solution on Pt electrodes. J Appl Electrochem, 2011;41:215-22.
[28] Jiang L, Hsu A, Chu D, Chen R. Ethanol electro-oxidation on Pt/C and PtSn/C catalysts in alkaline and acid solutions. Int J Hydrog Energ, 2010;35:365-72.
[29] Neto AO, Dias RR, Tusi MM, Linardi M, Spinacé EV. Electro-oxidation of methanol and ethanol using PtRu/C, PtSn/C and PtSnRu/C electrocatalysts prepared by an alcohol-reduction process. J Power Sources, 2007;166:87-91.
[30] Vigier F, Coutanceau C, Hahn F, Belgsir EM, Lamy C. On the mechanism of ethanol electro-oxidation on Pt and PtSn catalysts: Electrochemical and in situ IR reflectance spectroscopy studies. J Electroanal Chem. 2004;563:81-9.
[31] Lamy C, Rousseau S, Belgsir EM, Coutanceau C, Léger JM. Recent progress in the direct ethanol fuel cell: Development of new platinum-tin electrocatalysts. Electrochim Acta, 2004;49:3901-8.
[32] Baranova EA, Amir T, Mercier PHJ, Patarachao B, Wang D, Le Page Y. Single-step polyol synthesis of alloy Pt7Sn3 versus bi-phase Pt/SnOx nano-catalysts of controlled size for ethanol electro-oxidation. J Appl Electrochem, 2010;40:1767-77.
[33] Nieto-Márquez A, Romero R, Romero A, Valverde JL. Carbon nanospheres: Synthesis, physicochemical properties and applications. J Mater Chem, 2011;21:1664-72.

[34] Li W, Liang C, Zhou W, Qiu J, Zhou Z, Sun G, et al. Preparation and characterization of multiwalled carbon nanotube-supported platinum for cathode catalysts of direct methanol fuel cells. J Phys Chem B, 2003;107:6292-9.
[35] Darkrim F, Levesque D. High adsorptive property of opened carbon nanotubes at 77 K. J Phys Chem B, 2000;104:6773-6.
[36] De La Casa-Lillo MA, Lamari-Darkrim F, Cazorla-Amorós D, Linares-Solano A. Hydrogen storage in activated carbons and activated carbon fibers. J Phys Chem B, 2002;106:10930-4.
[37] Zheng Q, Wang D, Yuan F, Han Q, Dong Y, Liu Y, et al. An Effective Co-promoted Platinum of Co–Pt/SBA-15 Catalyst for Selective Hydrogenation of Cinnamaldehyde to Cinnamyl Alcohol. Catal Lett, 2016;146:1535-43.
[38] Lavin-Lopez MP, Paton-Carrero A, Sanchez-Silva L, Valverde JL, Romero A. Influence of the reduction strategy in the synthesis of reduced graphene oxide. Adv Powder Technol, 2017.
[39] Lavin-Lopez MP, Romero A, Garrido J, Sanchez-Silva L, Valverde JL. Influence of Different Improved Hummers Method Modifications on the Characteristics of Graphite Oxide in Order to Make a More Easily Scalable Method. Ind Eng Chem Res, 2016;55:12836-47.
[40] Jiménez V, Ramírez-Lucas A, Sánchez P, Valverde JL, Romero A. Improving hydrogen storage in modified carbon materials. Int J Hydrog Energ, 2012;37:4144-60.
[41] Lavin-Lopez M.P, Valverde JL, Dominguez-Delgado L. M., Sanchez-Silva L., Romero A. Enhancing the liquid phase exfoliation of graphite in both aqueous and organic mixtures. Int Research J Mat Sci and Appl. 2017;1:1-5.
[42] Díez-Ramírez J, Dorado F, De La Osa AR, Valverde JL, Sánchez P. Hydrogenation of CO2 to Methanol at Atmospheric Pressure over Cu/ZnO Catalysts: Influence of the Calcination, Reduction, and Metal Loading. Ind Eng Chem Res, 2017;56:1979-87.
[43] Brunauer S, Emmett PH, Teller E. Adsorption of gases in multimolecular layers. J Am Chem Soc, 1938;60:309-19.
[44] Barrett EP, Joyner LG, Halenda PP. The Determination of Pore Volume and Area Distributions in Porous Substances. I. Computations from Nitrogen Isotherms. J Am Chem Soc, 1951;73:373-80.
[45] Cheng LS. Improved Horvath—Kawazoe equations including spherical pore models for calculating micropore size distribution. Chem Eng Sci. 1994;49:2599-609.

[46] Díez-Ramírez J, Sánchez P, Rodríguez-Gómez A, Valverde JL, Dorado F. Carbon Nanofiber-Based Palladium/Zinc Catalysts for the Hydrogenation of Carbon Dioxide to Methanol at Atmospheric Pressure. Ind Eng Chem Res. 2016;55:3556-67.
[47] Nieto-Márquez A, Gil S, Romero A, Valverde JL, Gómez-Quero S, Keane MA. Gas phase hydrogenation of nitrobenzene over acid treated structured and amorphous carbon supported Ni catalysts. App Catal A-Gen, 2009;363:188-98.
[48] de la Osa AR, Romero A, Dorado F, Valverde JL, Sánchez P. Influence of cobalt precursor on efficient production of commercial fuels over FTS Co/SiC catalyst. Catalysts. 2016;6.
[49] Lobato J, Zamora H, Plaza J, Rodrigo MA. Composite Titanium Silicon Carbide as a Promising Catalyst Support for High-Temperature Proton-Exchange Membrane Fuel Cell Electrodes. Chem Cat Chem, 2016;8:848-54.
[50] Lobato J, Zamora H, Plaza J, Cañizares P, Rodrigo MA. Enhancement of high temperature PEMFC stability using catalysts based on Pt supported on SiC based materials. Appl Catal B-Environ, 2016;198:516-24.
[51] Lasch K, Hayn G, Jörissen L, Garche J, Besenhardt O. Mixed conducting catalyst support materials for the direct methanol fuel cell. J Power Sources, 2002;105:305-10.
[52] Rizo R, Sebastián D, Lázaro MJ, Pastor E. On the design of Pt-Sn efficient catalyst for carbon monoxide and ethanol oxidation in acid and alkaline media. Appl Catal B-Environ, 2017;200:246-54.
[53] Ghaemi F, Abdullah LC, Rahman NMANA, Najmuddin SUFS, Abdi MM, Ariffin H. Synthesis and comparative study of thermal, electrochemical, and cytotoxicity properties of graphene flake and sheet. Res Chem Intermediat, 2017;43:4981-91.
[54] Soni KC, Krishna R, Chandra Shekar S, Singh B. Catalytic oxidation of carbon monoxide over supported palladium nanoparticles. Appl Nanosci, 2016;6:7-17.
[55] Abdel Hameed RM, Fetohi AE, Amin RS, El-Khatib KM. Promotion effect of manganese oxide on the electrocatalytic activity of Pt/C for methanol oxidation in acid medium. Appl Surf Sci, 2015;359:651-63.
[56] Antolini E. Catalysts for direct ethanol fuel cells. J Power Sources, 2007;170:1-12.
[57] Riad M, Saad L, Mikhail S. Influence of Support Type on the Pore Structure and Catalytic Activity of Pt-Sn/ Alumino-Silicate Catalysts. Australian Journal of Basic and Applied Sciences. 2008;2:262-71.
[58] Serp P, Machado B. Nanostructured Carbon Materials for Catalysis 2015.

[59] Schonvogel D, Hülstede J, Wagner P, Kruusenberg I, Tammeveski K, Dyck A, et al. Stability of Pt Nanoparticles on Alternative Carbon Supports for Oxygen Reduction Reaction. J Electrochem Soc, 2017;164:F995-F1004.
[60] Xu ZJ. From Two-Phase to Three-Phase: The New Electrochemical Interface by Oxide Electrocatalysts. Nano-Micro Lett, 2017;10:8.
[61] Zamora H, Plaza J, Velhac P, Cañizares P, Rodrigo MA, Lobato J. SiCTiC as catalyst support for HT-PEMFCs. Influence of Ti content. Appl Catal B-Environ, 2017;207:244-54.
[62] Khotseng L, Bangisa A, Modibedi RM, Linkov V. Electrochemical Evaluation of Pt-Based Binary Catalysts on Various Supports for the Direct Methanol Fuel Cell. Electrocatal, 2016;7:1-12.
[63] Baranova EA, Le Page Y, Ilin D, Bock C, MacDougall B, Mercier PHJ. Size and composition for 1–5nm Ø PtRu alloy nano-particles from Cu Kα X-ray patterns. J Alloys Compd, 2009;471:387-94.
[64] Li H, Sun G, Cao L, Jiang L, Xin Q. Comparison of different promotion effect of PtRu/C and PtSn/C electrocatalysts for ethanol electro-oxidation. Electrochim Acta, 2007;52:6622-9.
[65] Kim JH, Choi SM, Nam SH, Seo MH, Choi SH, Kim WB. Influence of Sn content on PtSn/C catalysts for electrooxidation of C1-C3 alcohols: Synthesis, characterization, and electrocatalytic activity. Appl Catal B-Environ, 2008;82:89-102.
[66] Bergeret G, Gallezot P. Particle size and dispersion measurements. Handbook of Heterogeneous Catalysis: Online. 2008:738-65.
[67] Ji Y, Cho Yi, Jeon Y, Lee C, Park D-H, Shul Y-G. Design of active Pt on TiO2 based nanofibrous cathode for superior PEMFC performance and durability at high temperature. Appl Catal B-Environ, 2017;204:421-9.
[68] Miranzo P, Ramírez C, Román-Manso B, Garzón L, Gutiérrez HR, Terrones M, et al. In situ processing of electrically conducting graphene/SiC nanocomposites. J Eur Ceram Soc, 2013;33:1665-74.
[69] Pantea D, Darmstadt H, Kaliaguine S, Roy C. Electrical conductivity of conductive carbon blacks: influence of surface chemistry and topology. Appl Surf Sci, 2003;217:181-93.
[70] Jiang L, Sun G, Zhou Z, Zhou W, Xin Q. Preparation and characterization of PtSn/C anode electrocatalysts for direct ethanol fuel cell. Catal Today, 2004;93-95:665-70.

[71] Tayal J, Rawat B, Basu S. Bi-metallic and tri-metallic Pt-Sn/C, Pt-Ir/C, Pt-Ir-Sn/C catalysts for electro-oxidation of ethanol in direct ethanol fuel cell. Int J Hydrog Energ, 2011;36:14884-97.
[72] Liu F, Yi B, Xing D, Yu J, Hou Z, Fu Y. Development of novel self-humidifying composite membranes for fuel cells. J Power Sources, 2003;124:81-9.
[73] Mamlouk M, Scott K. Analysis of high temperature polymer electrolyte membrane fuel cell electrodes using electrochemical impedance spectroscopy. Electrochim Acta, 2011;56:5493-512.
[74] Ju H, Giddey S, Badwal SPS. The role of nanosized SnO2 in Pt-based electrocatalysts for hydrogen production in methanol assisted water electrolysis. Electrochim Acta, 2017;229:39-47.